

EPR studies of manganese centers in SrTiO₃: Non-Kramers Mn³⁺ ions and spin-spin coupled Mn⁴⁺ dimers

D V Azamat¹, A Dejneka¹, J Lancok¹, V A Trepakov^{1,2}, L Jastrabik¹
and A G Badalyan²

¹ Institute of Physics AS CR, 182 21, Prague 8, Czech Republic

² Ioffe Physical-Technical Institute, Russian Academy of Sciences, 194021, St. Petersburg, Russia

E-mail: azamat@fzu.cz

Abstract

X- and Q-band electron paramagnetic resonance (EPR) study is reported on the SrTiO₃ single crystals doped with 0.5-at.% MnO. EPR spectra originating from the $S = 2$ ground state of Mn³⁺ ions are shown to belong to the three distinct types of Jahn-Teller centres. The ordering of the oxygen vacancies due to the reduction treatment of the samples and consequent formation of oxygen vacancy associated Mn³⁺ centres are explained in terms of the localized charge compensation. The EPR spectra of SrTiO₃: Mn crystals show the presence of next nearest neighbor exchange coupled Mn⁴⁺ pairs in the $\langle 110 \rangle$ directions.

Keywords: A. inorganic compounds; D. electron paramagnetic resonance (EPR); D. magnetic properties

1. Introduction

Transition metal doped perovskites has attracted increasing interest due to a variety of physical phenomena such as superconductivity, colossal magnetoresistance and metal-to-insulator transition [1-4]. Strontium titanate, the so called incipient ferroelectric with perovskite structure, has become in the focus of interest in attempt to combine magnetic and ferroelectric properties of the material [5-11]. In this work we use EPR spectroscopy for the accurate determination of different oxidation states and local

environment of manganese impurities in SrTiO₃. Trivalent manganese ions in SrTiO₃ crystals look like a model ones to study exchange-coupled systems in mixed-valent manganese oxides [12-17]. EPR spectra of Mn³⁺ complexes in oxide crystals have been poorly [18, 19] investigated than those of 3d⁴ non-Kramers iron (Fe⁴⁺ ions) [20-22]. These ions exhibit large zero field splittings due to the influence of the Jahn-Teller effect on the ⁵E_g ground state in octahedral symmetry. An EPR centre attributed to the Mn³⁺-V_O complex was reported by Serway et al [19], only the transition within $M_S = 2 \leftrightarrow M_S = -2$ states of electron spin $S = 2$ system was observed. A strong axial field is created by a nearest-neighbour oxygen vacancy V_O. So far, the lack of information on the Mn³⁺ centres in SrTiO₃ has precluded the detailed analysis for that system. Owing to the large interest in the characterisation of Mn³⁺ complexes in perovskites, we decided to perform EPR study on this system.

In this paper we report X- and Q-band EPR measurements on SrTiO₃: Mn single crystals. The EPR spectrum of SrTiO₃ crystals doped with manganese contains resonances from cubic Mn⁴⁺ and Mn²⁺ ions as well as from several types of Mn³⁺ centres. The accurate values of the 2-nd and 4-th rank crystal field tensor components have been obtained for distinct types of Mn³⁺ centres. The peculiar features of Mn³⁺ centres were established by the studies of hyperfine interaction with 100% abundant ⁵⁵Mn nuclei (nuclear spin of $I = 5/2$). The spectra of distinct types of Mn³⁺ centres differ greatly in the magnitude of their ⁵⁵Mn hyperfine fields.

The careful analysis of spin-spin coupling effects may provide some useful physical information on structural and electronic properties of SrTiO₃. When crystals of SrTiO₃ are heavily doped with fourvalent manganese there is a tendency for the Mn⁴⁺ ions to form exchange coupled pairs. The EPR spectra indicate the formation of Mn⁴⁺ dimer centers lying along the <110> directions (in the next nearest neighbor position). The coupling in the ground state is expected to be ferromagnetic.

2. Experimental procedure

The single crystals of SrTiO₃ were grown in Furuuchi Chemical Corporation by use of Verneuil technique through the melting of SrTiO₃ and 0.5% wt of MnO crystalline powders. Some of the samples were annealed for 6 h at 1000 C in Ar/H₂ (5%) reduction atmosphere. EPR measurements were performed with a Bruker ELEXSYS 580 spectrometer at X- and Q-band frequencies in the temperature range 65-300K.

3. Results and Discussion

3.1. Non-Kramers Mn³⁺ ions

In addition to the cubic Mn^{4+} ($3d^3$) and Mn^{2+} ($3d^5$) spectra, that are already known, the spectra of strong axially distorted Mn^{3+} ($3d^4$) ions have been found (see Fig. 1). These manganese centers as well as a variety of the other $3d$ impurities in SrTiO_3 are typically substituted for Ti^{4+} sites in the octahedral coordination [11, 19, 23-25].

Table 1. The Spin Hamiltonian parameters of Mn^{3+} centres in SrTiO_3 single crystals (in 10^{-4} cm^{-1} , 295K).

centre	b_2^0	b_4^0	b_4^4	g_{\parallel}	g_{\perp}	A_{\parallel}	A_{\perp}
$\text{Mn}^{3+}\text{-V}_O$ (I)	28440.0	170.0	-3800.0	1.986	1.997	-38.0	-64.0
$\text{Mn}^{3+}\text{-X}$	27550.0	170.0	-1350.0	1.986	1.997	-10.4	-29.8
$\text{Mn}^{3+}\text{-V}_O$ (II)	26340.0	170.0	-1350.0	1.986	1.997	-28.0	-45.0

Practically, the studies of the angular dependencies of EPR spectra reveal three types of the Mn^{3+} centers with the spin $S = 2$. These centers has axial symmetry with the main axis along to the [100]-type directions.

Figure 2 shows the axial Mn^{3+} centres for applied magnetic field direction $B_{\parallel}[100]$. The Mn^{3+} spectra consists of $2 \leftrightarrow -2$ and $1 \leftrightarrow -1$ fine structure transitions within 5B_1 ground state. We use the following spin Hamiltonian with symmetry D_{4h} to describe the ground state energy splitting of Mn^{3+} centres:

$$H = g_{\parallel}\beta_e B_z S_z + g_{\perp}\beta_e (B_x S_x + B_y S_y) + B_{20}\bar{O}_0^2 + B_{40}\bar{O}_0^4 + B_{44}\bar{O}_4^4 + A_{\parallel}S_z I_z + A_{\perp}(S_x I_x + S_y I_y) \quad (1)$$

$$\bar{O}_0^l = T_0^l, \quad \bar{O}_m^l = T_{-m}^l + (-1)^m T_m^l$$

where $S = 2$, the first two terms describes the Zeeman interaction, the last two ones correspond to the hyperfine (HF) interactions; β_e is the Bohr magneton; g is the g-tensor; A is the hyperfine (HF) interaction tensor; $B_{20} = \frac{2}{\sqrt{6}}b_2^0$, $B_{40} = \frac{\sqrt{70}}{30}b_4^0$, $B_{44} = \frac{1}{30}b_4^4$ are the scalar fine structure constants; T_m^l are spherical tensor operators [28] and b_l^m are Stevens coefficients; x, y, z , the crystallographic axes.

Figure 3 shows the angular variation of the spectra measured in the (100) plane at the temperature $T=150\text{K}$. The magnetic multiplicity of EPR spectra $K_M = 3$ corresponds with three possible axial distortions along [100] type of directions. The curves on Fig. 3 have been calculated by diagonalization of the spin Hamiltonian (1) by using a program similar to that described in [28]. The characteristic EPR road map has shown just for centers designated as $\text{Mn}^{3+}\text{-V}_\text{O}$ (II) because the corresponding fine structure transitions of $\text{Mn}^{3+}\text{-V}_\text{O}$ (I) and $\text{Mn}^{3+}\text{-X}$ centers follows nearby through the complete angular dependence. The parameters of the spin Hamiltonian (1) for the $\text{Mn}^{3+}\text{-V}_\text{O}$ (I), $\text{Mn}^{3+}\text{-X}$ and $\text{Mn}^{3+}\text{-V}_\text{O}$ (II) centers are listed in Table 1. In Fig. 4 it is shown the hyperfine structure of Mn^{3+} spectra are well resolved at the temperature of 295K and has narrow resonance linewidths of about 1.2 mT. The Mn^{3+} hyperfine interaction is axially symmetric around a [100] direction as well as g-tensor main axis. The weaker HF interaction is for parallel magnetic-field orientation with respect to the tetragonal axis of the center (the local z axis), while the stronger HF interaction is in the equatorial plane perpendicular to the local z axis of the center.

High spin Mn^{3+} free ion term is 5D in octahedral environment. It gives 5E ground state that is not split by spin-orbit coupling at first order of perturbation theory [26, 27]. A strong axial field results in lowering the symmetry to D_{4h} . This give rise to $S = 2$ high spin configuration $(t_{2g})^3(e_g)^1$ with an orbital singlet 5B_1 ($3z^2-r^2$) ground state. The stabilization of ground state $3d(3z^2-r^2)$ orbital results in the shift the four oxygen ions in the equatorial plane towards the central Mn^{3+} ion and the moving of two oxygen ions away making elongated octahedral. The inspection of the values of hyperfine structure constants (see Table 1) of the centers show that although the ground state $S = 2$ is the same as that for Mn^{3+} the actual spin density of different types of the centers is rather delocalized among surrounding ions due to strong covalent bonding. The anisotropic hyperfine splitting for the 5B_1 state of different types of Mn^{3+} centers can be evaluated by use of the values from Table 1. For an $3d(3z^2-r^2)$ ground state the relations are the following [26, 29-32]:

$$A_{\parallel} = \frac{1}{7}P - a + P\Delta g_{\parallel}, \quad A_{\perp} = -\frac{1}{14}P - a + P\Delta g_{\perp}, \quad (2a)$$

$$P = g_e g_N \beta_e \beta_N \langle r^{-3} \rangle,$$

$$\chi = \frac{4\pi}{S} \langle \psi | \sum_i \delta(r_i) s_{zi} | \psi \rangle = -\frac{3}{2} \left(\frac{hca_0^3}{g_e g_N \beta_e \beta_N} \right) a, \quad (2b)$$

where isotropic contact term χ is the value of the density of unpaired spins at the nucleus; the \parallel and \perp symbols denote the parallel and perpendicular components of HF interaction tensor with respect to the local z axis of the center. Because the g_{\parallel} and A_{\parallel} parameters are smaller than g_{\perp} and A_{\perp} (see Table 1) the ground state $3d(3z^2-r^2)$ orbital is more likely rather than $3d(x^2-y^2)$. The adoption of negative signs of

hyperfine interaction constants (see Table 1) is a reasonable choice which leads to negative contact term χ coming from the core polarization. By use of the data in Table 1 we find the values of P , a and χ listed in the Table 2 (as evaluated by use of formulae (2)). The P value for Mn^{3+} -X centre is appreciably smaller than for Mn^{3+} - V_O (I, II) ones. The Mn^{3+} HF interaction data in SrTiO_3 yields quite different magnitudes of hyperfine structure constants from that found for Mn^{3+} complexes in titanium oxide (TiO_2) crystals [12]. The essential reduction of contact interaction χ values exhibits the strong covalent bonding of the Mn^{3+} impurities. The main contribution to the contact term comes from the spin polarization of the core s -shells due to the exchange interaction with the d -electron spin states [33, 34].

Let us consider the possible microscopic models of Mn^{3+} centers (see Fig. 5) based on the present experimental data. All the spectra are characterized by $g_{\parallel} < g_{\perp} < 2$ in the cubic phase. Therefore it results from ${}^5B_1(3z^2-r^2)$ state of Mn^{3+} ion in the presence of a strong positive axial crystal field. All the Mn^{3+} centers are very stable at room temperature. The dominant charge compensation process for Mn^{3+} ions is the formation of the oxygen vacancies at the nearest or next nearest anionic positions along [100] type of directions.

We suppose the Mn^{3+} - V_O (I) center is caused by an oxygen vacancy V_O in immediate neighborhood of the Mn^{3+} ion where empty oxygen vacancy stabilize a $3d(3z^2-r^2)$ orbital of Jahn-Teller active defect. Thus, the EPR spectra of Mn^{3+} - V_O (I) ions of axial symmetry are analogous to the corresponding spectra of Fe^{3+} with an oxygen vacancy in the nearest environment [35]. Other example of nearest V_O charge compensated defect is Ni^{3+} - V_O [36]. The EPR transitions within the $|\pm 2\rangle$ non-Kramers doublet of Mn^{3+} - V_O (I) pair centers with the nearest neighbor oxygen vacancy was observed for the first time by Serway et al [19].

It should be pointed out the relative concentrations of the Mn^{3+} - V_O (I) and Mn^{3+} - V_O (II) centers depend on the thermal treatment of the sample in reduced atmosphere. Figure 4 shows the EPR spectra corresponds with $1 \leftrightarrow -1$ transition of as grown and additionally reduced manganese-doped SrTiO_3 with the applied magnetic field parallel to the [110] axis. The relative change of EPR intensity of Mn^{3+} - V_O (I) and Mn^{3+} - V_O (II) centers due to additional reduction of the samples supports to conclusion that the charge compensators like oxygen vacancies are mobile defects in respect to the Mn^{3+} sites (under annealing process).

Table 2. Hyperfine coupling parameters of Mn^{3+} centres in SrTiO_3 and TiO_2 single crystals

centre	$10^4 P$ (cm^{-1})	$10^4 a$ (cm^{-1})	χ (a.u.)	ref.
--------	-------------------------------	-------------------------------	---------------	------

SrTiO ₃ : Mn ³⁺ -V _O (I)	121.3	55.3	-1.88	*
SrTiO ₃ : Mn ³⁺ -X	90.5	23.3	-0.79	*
SrTiO ₃ : Mn ³⁺ - V _O (II)	79.3	39.3	-1.33	*
TiO ₂ : Mn ³⁺	140.0	73.0	-2.45	[18]

* present study

We suppose, there is no oxygen vacancy V_O in the immediate neighborhood of the centers designated as Mn³⁺-V_O(II) in Table 1. In this case, a large axial field term results from a static Jahn-Teller distortion. In the SrTiO₃ structure the isolated oxygen vacancy has two nearest Ti⁴⁺ ions. The formation of neutral oxygen vacancies is accompanied by the trapping of two electrons [37]. In the case of the oxygen vacancy next nearest to Mn³⁺ ion the Mn³⁺- O- Ti³⁺- V_O complex is formed with axial distortion along [100] direction. This model is similar to that recently presented for Cr³⁺ charge compensated complex in SrTiO₃ [38]. Oxygen vacancy concentration could be increased by the annealing treatment of as grown sample in reducing atmosphere. Such procedure results in the relative increase of EPR signal of Mn³⁺- V_O (I) centers consisting of the nearest-neighbor neutrally charged oxygen vacancy (see Fig. 4). The main factors governing the distribution of trivalent Mn³⁺ impurities in the SrTiO₃ crystals appear to be electrostatic ones.

We propose the tentative model of Mn³⁺-X centers as Mn³⁺ nearest to Nb⁵⁺ ion substituted for Ti site. The Nb traces are than compensated by Mn³⁺ ions in the samples. A quite weak intensity of EPR signals of Mn³⁺-X centers is not visibly changed by the thermal treatment of the samples in reduced atmosphere. This is consistent with assumption that Mn³⁺ ion is a probable compensator for Nb⁵⁺ donor. Further experimental work shall concentrate on the Mn³⁺-X center to confirm the model suggested by the present study.

3.2. Exchange-coupled Mn⁴⁺ pairs

In as grown crystals the cubic Mn⁴⁺ (as well as cubic Mn²⁺) dominates EPR spectrum which indicates that the majority of the Mn⁴⁺ ions enter the lattice as isolated centres. The EPR of isolated Mn⁴⁺ ions have been described [24] by the spin Hamiltonian for a 3d³ electron system ($I=5/2$) in octahedral environment:

$$H_i = g\beta\mathbf{B} \cdot \mathbf{S} + D_c \left[\mathbf{S}_z^2 - \frac{1}{3} \mathbf{S}(\mathbf{S} + 1) \right] + \mathbf{A} \mathbf{S} \cdot \mathbf{I}, \quad (3)$$

where the axial zero-field splitting $D_c \sim 0$ at room temperature and therefore EPR spectrum is almost isotropic. The spin Hamiltonian parameters are given in Table 3. When two Mn^{4+} ions with electron spin $S=3/2$ are spin-spin coupled the dimer spin states are characterized by the total spin quantum number $\Sigma = \mathbf{S}_1 + \mathbf{S}_2 = 0, 1, 2, 3$ [26, 32, 39]. The EPR spectra of SrTiO_3 crystals heavily doped with $\text{Mn}^{4+}_{\text{Ti}}$ ($3d^3$) contain resonance lines which can be assigned to the total electron spin quantum number $\Sigma = 1$ of exchange-coupled pair. Figure 2 show the spectrum of Mn^{4+} - Mn^{4+} in SrTiO_3 under applied magnetic field parallel to [100] direction. The isolated ion spectrum of Mn^{4+} is very much more intense than the pair spectrum. Suggesting the isotropic part of exchange energy is large compared to the other magnetic interactions the X-band EPR angular dependence from the $\Sigma = 1$ state can be well described by the spin Hamiltonian [39]:

$$H = \beta \mathbf{B} \cdot \mathbf{g} \cdot \Sigma + D_\Sigma \left[\Sigma_z^2 - \frac{1}{3} \Sigma(\Sigma + 1) \right] + E_\Sigma \left[\Sigma_x^2 - \Sigma_y^2 \right] + \Sigma \cdot \mathbf{A} \cdot (\mathbf{I}_1 + \mathbf{I}_2), \quad (4a)$$

$$D_\Sigma = 3\alpha_\Sigma D_e + \beta_\Sigma D_c, \quad E_\Sigma = \alpha_\Sigma E_e + \beta_\Sigma E_c, \quad \alpha_1 = 17/10, \quad \beta_1 = -12/5 \quad (4b)$$

where Σ represent spin operators for the exchange-coupled Mn^{4+} ions, the first term describe the electron Zeeman interaction, the second and third ones describes the axial and orthorhombic second rank fine splitting, A are the magnetic hyperfine interaction constants of the 100% abundant isotope ^{55}Mn , $I_1=I_2=5/2$. The main axes z , x and y of second rank fine structure tensor are parallel to $[110]$, $[\bar{1}10]$ and $[001]$ directions respectively. If the Mn^{4+} is located along a $[110]$ direction relative to the other substitutional Mn^{4+} ion than it generates an orthorhombic field and is related to six other symmetry conjugated sites. The spin Hamiltonian parameters for the $\Sigma = 1$ transitions presented in Table 3 were derived from angular dependences of EPR spectra recorded with the magnetic field varied in (100) and (110) planes. As shown on Fig. 6 the angular dependence of $\Sigma = 1$ is strongly defined by the both D_l and E_l terms. We have found that $E_l / D_l \approx 1/3$ that means there is maximum rhombic splitting and the components of corresponding Cartesian second rank fine tensor \mathbf{D} are the following [26]:

$$D_{xx} = -\frac{D_1}{3} + E_1 \approx 0, \quad D_{yy} = -\frac{D_1}{3} - E_1 \approx -\frac{2D_1}{3}, \quad D_{zz} = \frac{2D_1}{3} \quad (5)$$

For this dimer centers which exhibits isotropic g-factor the anisotropy of exchange interaction is mainly caused by dipole-dipole interaction. If we adopt the point dipole approximation for the Mn^{4+} ions constituting the pair then the value of D_e is defined as follows: $D_e = -g^2 \beta^2 / R^3$, where R is interionic distance. By use of formulas (4b) and suggesting that axial splitting of isolated Mn^{4+} ion $D_c \sim 0$ we obtain

the room temperature value of $D_e \sim 0.0147 \text{ cm}^{-1}$ and corresponding distance of approximately 4.9 \AA . This value is significantly reduced from the separation of $\sim 5.5 \text{ \AA}$ between nearest regular Ti^{4+} sites located along $\langle 110 \rangle$ direction. These findings are confirmed experimentally by the observation of characteristic hyperfine structure of the exchange-coupled pair complexes as shown on Fig.7. The hyperfine structure consist of 11 lines with hyperfine splitting constant half that of the isolated Mn^{4+} ions and with intensity ratio 1:2:3:4:5:6:5:4:3:2:1 expected for identical Mn^{4+} ions coupled by an isotropic exchange interaction larger than the hyperfine interaction. The intensities of the $\Sigma = 1$ transitions are difficult to follow as a function of temperature and therefore the energy intervals between the spin states Σ were not evaluated.

Table 3. The Spin Hamiltonian parameters of single Mn^{4+} centres and Mn^{4+} - Mn^{4+} ($\Sigma = 1$) exchange-coupled pairs in SrTiO_3 single crystals (in 10^{-4} cm^{-1}), $T=295\text{K}$.

centre	$D_{\Sigma=1}$	$E_{\Sigma=1}$	g	A	ref.
Mn^{4+}	-	-	1.994	-69.4	[24]
Mn^{4+} - Mn^{4+}	-750.0	-248.0	1.994	-34.7	*

* present study

The analysis of the angular variation of EPR spectra of Mn^{4+} dimers provides a basis for constructing the model of exchange coupled pairs in SrTiO_3 lattice. The structure of next nearest neighbor pair site, shown on Fig. 8, has point group symmetry D_{2h} in a cubic phase of SrTiO_3 . The pairs consist of two Mn^{4+} ions which are substituted for nearest Ti^{4+} sites located along one of the $\langle 110 \rangle$ crystal directions. These measurements do not provide complete information related to the energy level sequence of Mn^{4+} - Mn^{4+} pairs but the data obtained do suggest that the $\Sigma = 1$ state is higher in energy in comparison to the other $\Sigma = 2, 3$ states. The magnetic interactions must be transmitted through pathways involving three intervening ions: one titanium and two oxygen atoms. In this case ferromagnetic right angle superexchange interaction is expected because of Mn-O bonds in perovskite structure.

4. Conclusions

The detailed studies have performed on the several complexes of high spin Mn^{3+} ions. We were able to define the sign and value of the axial fine structure parameters b_2^0 that is important to elucidate the defect

structure at the Mn^{3+} site. The tetragonally elongated octahedron coming from Jahn-Teller distortions of a local site of Mn^{3+} centers have been ascertained from EPR data. Spin density at the nucleus for manganese in the distorted octahedral coordination has been found considerably different for various types of the centers. A variety of complex Mn^{3+} ions detected in SrTiO_3 crystals has been ascribed to differences in charge compensation. These variations are largely due to the techniques used to grow and dope the SrTiO_3 single crystals. Our results show the formation of exchange coupled Mn^{4+} dimers substituted for the second nearest neighbor Ti^{4+} sites in SrTiO_3 crystals.

Acknowledgements

This work was supported by the Operational Program Research and Development for Innovations - European Social Fund (project CZ.1.05/2.1.00/03.0058 of the Ministry of Education, Youth and Sports of the Czech Republic), project SAFMAT CZ.2.16/3.1.00/22132, grant 202/09/J017 of GACR and grant No. 01010517 of the TACR, by the PP RAS "Quantum physics of condensed Matter" and by the RFBR No. 12-02-00848, by the Ministry of Education and Science under Contract No. 14.740.11.0048, by the programs of RAS: "Spintronics".

References

- [1] Bednorz J G and Müller K A 1986 Z. Phys. B: Condens. Matter **64** 189
- [2] von Helmolt R, Wecker J, Holzappel B, Schultz L and Samwer K 1993 Phys. Rev. Lett. **71** 2331
- [3] Imada M, Fujimori A and Tokura Y 1998 Rev. Mod. Phys. **70** 1039
- [4] Waser R and Aono M 2007 Nature Mater. **6** 833
- [5] Alvarado S F, La Mattina F and Bednorz J G 2007 Appl. Phys. A: Mater. Sci. Process. **89** 85
- [6] La Mattina F, Bednorz J G, Alvarado S F, Shengelaya A and Keller H 2008 Appl. Phys. Lett. **93** 022102
- [7] Khomskii D 2009 Physics **2** 20
- [8] Nagaev E L 2001 Phys. Rep. **346** 387
- [9] Savinov M, Trepakov V A, Syrnikov P P, Zelezny V, Pokorny J, Dejneka A, Jastrabik L and Galinetto P 2008 J. Phys. Condens. Matter **20** 095221
- [10] Badalyan A G, Syrnikov P P, Azzoni C B, Galinetto P, Mozzati M C, Rosa J, Trepakov V A and Jastrabik L 2008 J. Appl. Phys. **104** 033917
- [11] Müller K A and Fayet J C 1991 *Structural Phase Transitions II* eds K A Müller and H Thomas (Berlin-Heidelberg: Springer) pp 1-82
- [12] Kanamori J 1959 J. Phys. Chem. Solids **10** 87

- [13] Shengelaya A, Zhao Guo-meng, Keller H, Müller K A and Kochelaev B I 2000 Phys. Rev. B **61** 5888
- [14] Coey J M D, Viret M and von Molnár S 1999 Adv. Phys. **48** 167
- [15] Dagotto E, Hotta V and Moreo A 2001 Phys. Rep. **344** 1
- [16] Kvyatkovskii O E 2011 Crystallogr. Rep. **56** 3
- [17] Inoue J 1998 Phil. Trans. R. Soc. Lond. A **356** 1481
- [18] Gerritsen H J and Sabisky F S 1963 Phys. Rev. **132** 1507
- [19] Serway R A, Berlinger W, Müller K A and Collins R W 1977 Phys. Rev. B **16** 4761
- [20] Schirmer O F, Berlinger W and Müller K A 1975 Solid State Commun. **16** 1289
- [21] Faust B, Reyher H-J, Schirmer O F 1996 Solid State Commun. **98** 445
- [22] Azamat D V, Basun S A, Bursian V E, Razdobarin A G, Sochava L S, Hesse H and Kapphan S 1999 Phys. Solid State **41** 1303
- [23] Blazey K W, Cabrera J M and Müller K A 1983 Solid State Commun. **45** 903
- [24] Müller K A 1959 Phys. Rev. Lett. **2** 341
- [25] Müller K A 1981 J. Phys. (Paris) **42** 551
- [26] Abragam A and Bleaney B 1970 *Electron Paramagnetic Resonance of Transition Ions* (Oxford: Clarendon)
- [27] Griffith J S 1964 *The Theory of Transition-Metal Ions* (London: Cambridge University)
- [28] Grachev V G 1987 Sov. Phys. JETP **65** 1029
- [29] Abragam A and Pryce M H L 1951 Proc. Roy. Soc. (London) **206** 135
- [30] McGarvey B R 1967 J. Phys. Chem. **71** 51
- [31] McGarvey B R 1966 *Transition Metal Chemistry* vol 3, ed R L Carlin (New York: Marcel Dekker) pp 90-201
- [32] Al'tshuler S A and Kozyrev B M 1974 *Electron Paramagnetic Resonance in Compounds of Transition Elements* (New York: Wiley)
- [33] Watson R E and Freeman A J 1967 *Hyperfine interactions* eds A J Freeman and R B Frankel (New York – London: Academic Press) pp 53-94
- [34] Simanek E and Müller K A 1970 J. Phys. Chem. Solids **31** 1027
- [35] von Waldkirch Th, Müller K A and Berlinger W 1972 Phys. Rev. B **5** 4324
- [36] Müller K A, Berlinger W and Rubins R S 1961 Phys. Rev. **186** 361
- [37] Ricci D, Bano G and Pacchioni G 2003 Phys. Rev B **68** 224105
- [38] La Mattina F, Bednorz J G, Alvarado S F, Shengelaya A, Müller K A and Keller H 2009 Phys. Rev. B **80** 075122

[39] Owen J and Harris E A 1972 *Electron Paramagnetic Resonance* ed S Geschwind (New York: Plenum Press) pp 427-492

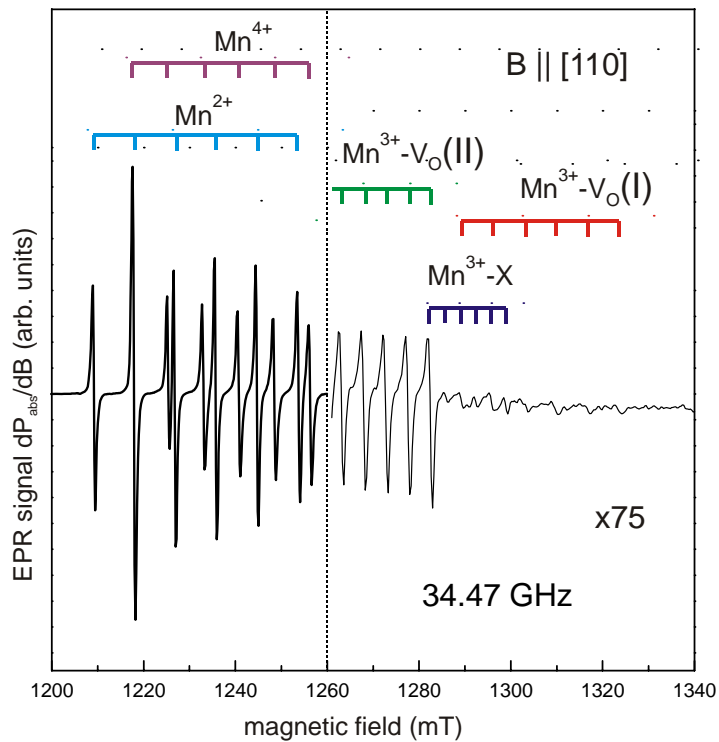


Figure 1. Q-band EPR spectra of $SrTiO_3:Mn$ showing the cubic Mn^{4+} and Mn^{2+} as well as charge compensated Mn^{3+} ions. $B \parallel [100]$, $T = 295K$. EPR spectrum of axial Mn^{3+} centres is enlarged by x75 in comparison to one of the cubic Mn^{4+} and Mn^{2+} . The resolved hyperfine structure shown by the cropped lines is due to the interaction with the ^{55}Mn nuclei.

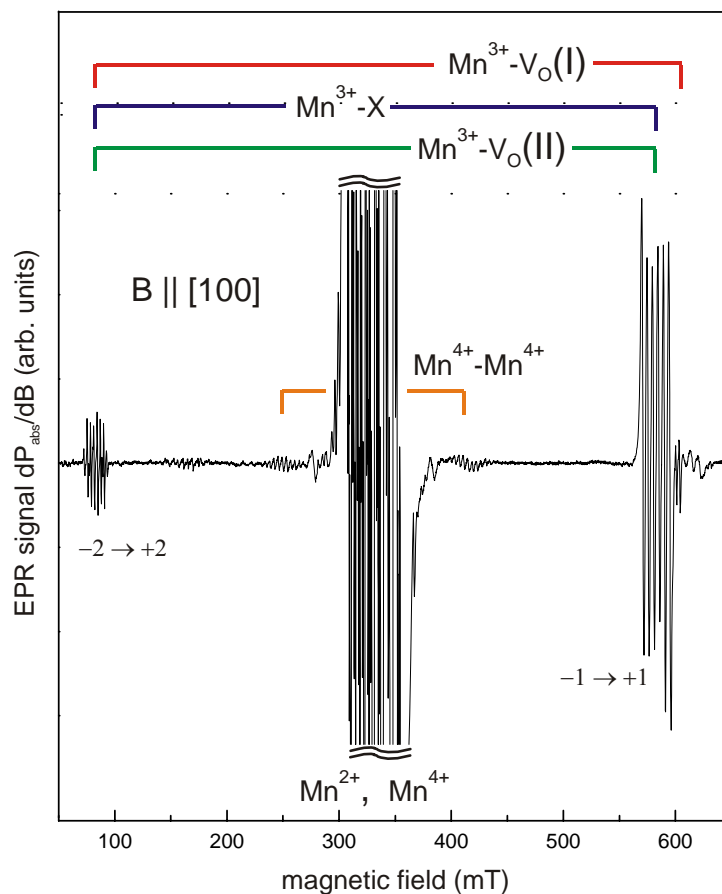


Figure 2. X-band EPR spectrum of the charge compensated Mn^{3+} ions and Mn^{4+} dimers when applied magnetic field parallel to $[100]$ direction, microwave frequency of 9.24 GHz, $T = 295K$. EPR spectra of cubic Mn^{2+} and Mn^{4+} ions are cut because of their extremely strong intensity. The fine structure transitions are shown by the cropped lines.

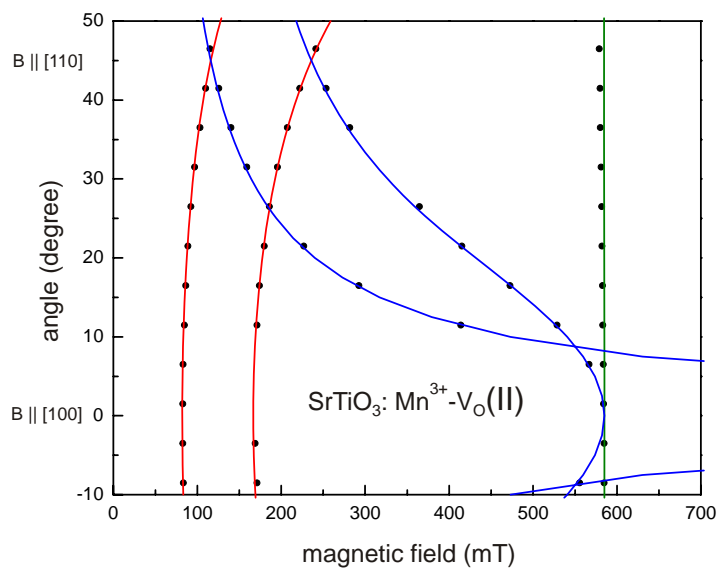


Figure 3. The EPR road map of the center of gravity of Mn³⁺-V_O(II) resonance lines when applied magnetic field varies in the (100) plane, microwave frequency of 9.26 GHz, T = 150 K. The lines are the fine structure transitions calculated by exact diagonalization of spin Hamiltonian (1). The cycles show the experimental points.

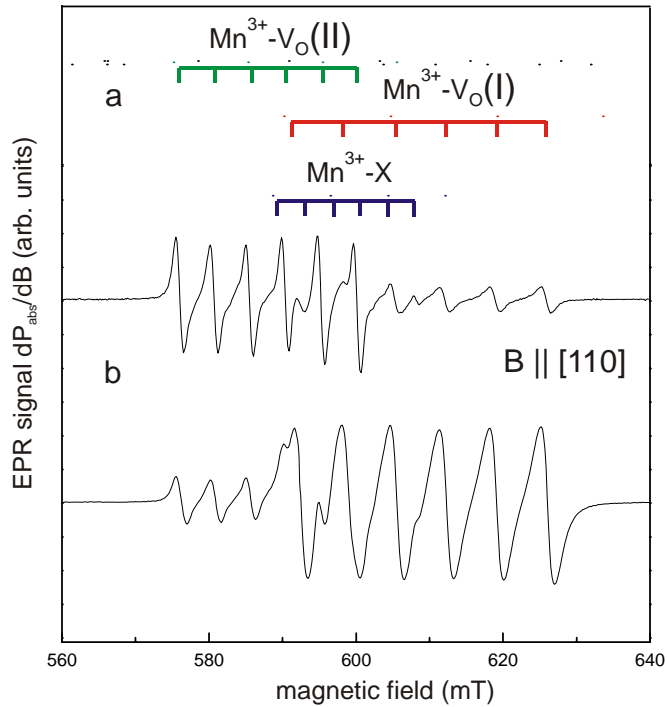


Figure 4. EPR spectrum of as grown (a) and additionally reduced (b) manganese-doped SrTiO₃ with the applied magnetic field parallel to the [110] axis, microwave frequency of 9.25 GHz, $T = 295$ K. The spectrum consists of lines corresponding to the $1 \leftrightarrow -1$ transition within 5B_1 ground state of distinct types of Mn³⁺ centers. The six fold splitting induced by the hyperfine interaction with the Mn nuclear spin $I = 5/2$ is shown by the cropped lines. The increase of intensity of Mn³⁺-V_O(I) resonance lines in comparison to Mn³⁺-V_O(II) once became apparent from these spectra.

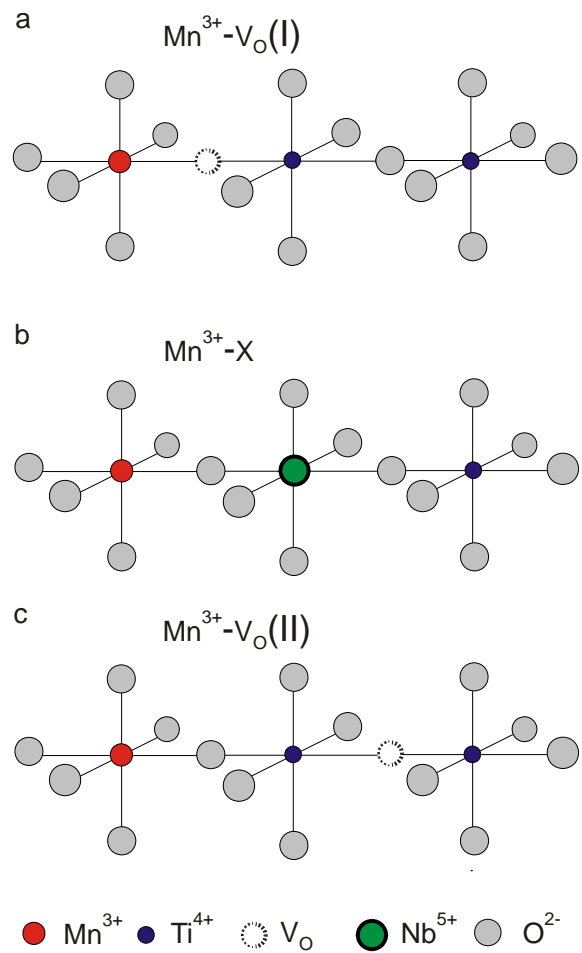


Figure 5. Possible models of charge compensated (a) $\text{Mn}^{3+}\text{-V}_\text{O}(\text{I})$, (b) $\text{Mn}^{3+}\text{-X}$ and (c) $\text{Mn}^{3+}\text{-V}_\text{O}(\text{II})$ centers in SrTiO_3 structure including the probable presence of a charge compensator along a $[100]$ direction in the first, second ($\text{Nb}^{5+}_{\text{Ti}}$) and third coordination sphere.

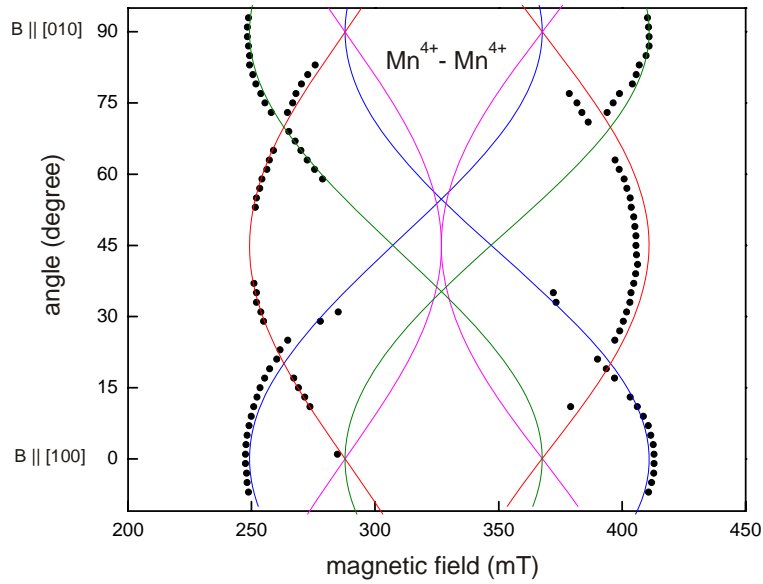


Figure 6. The road map of the center of gravity of EPR lines of $\Sigma = 1$ transitions from the Mn^{4+} - Mn^{4+} exchange-coupled pairs when applied magnetic field varies in the (100) plane, $T = 295$ K. The lines are the calculated positions of the resonances.

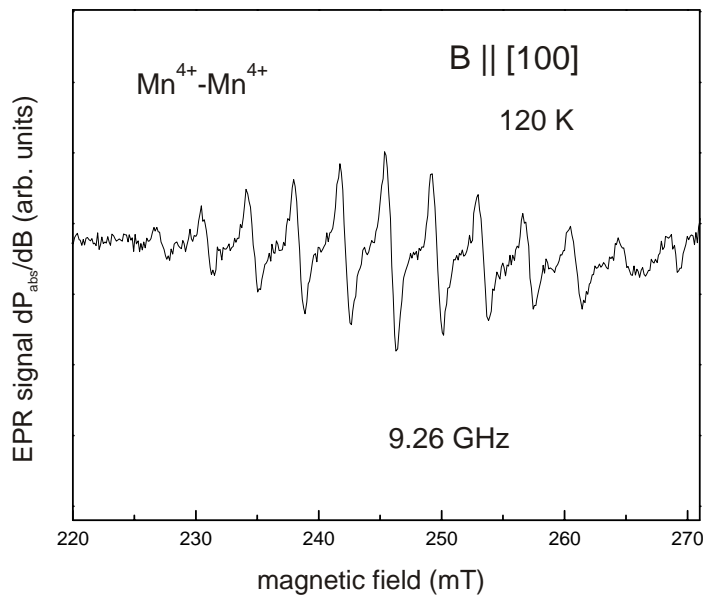


Figure 7. Hyperfine structure in the EPR spectrum of the next nearest neighbor exchange-coupled Mn^{4+} - Mn^{4+} pairs. This structure could be uniquely assigned to two equivalent Mn^{4+} ions ($I=5/2$).

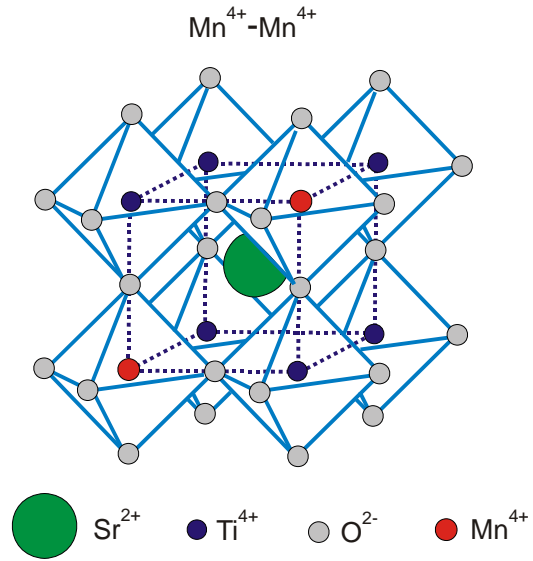


Figure 8. Model of exchange-coupled Mn^{4+} pairs in the cubic phase of SrTiO_3 with two Mn^{4+} ions which are substituted for nearest Ti^{4+} sites located along one of the $\langle 110 \rangle$ directions. The magnetic dipolar interaction between Mn^{4+} ions gives rise to anisotropy of exchange interaction.